Journal of Agricultural Science (2014), **152**, 817–828. © Cambridge University Press 2013
doi:10.1017/S0021859613000737

MODELLING ANIMAL SYSTEMS RESEARCH PAPER

Land usage classification: a hierarchical neural network approach

E. J. PALOMO[1]*, D. ELIZONDO[2] AND G. BRUNSCHWIG[3,4]

[1] *Department of Computer Science, University of Malaga, Malaga, Spain*
[2] *DIGITS, School of Computing and Informatics, Faculty of Technology, De Monfort University, Leicester, UK*
[3] *Clermont Université, VetAgro Sup, UMR1213 Herbivores, BP 10448, F-63000 Clermont-Ferrand, France*
[4] *INRA, UMR1213 Herbivores, Theix, F-63122 Saint-Genès Champanelle, France*

(*Received 29 May 2013; revised 9 August 2013; accepted 10 September 2013; first published online 23 October 2013*)

SUMMARY

The classification of land usage in mountain grassland bovine areas is important for the management of forage production and grazing in grass-based livestock systems. The present paper proposes a novel, hierarchical neural network-based approach towards the classification of land usage in these areas. A survey of 72 farms was conducted in the Massif Central (France). Information was gathered on geographical characteristics and cutting and/or grazing practices on three general groups of fields: cut only, cut and grazed and grazed only fields. To classify land usage, the data were clustered and visualized in a hierarchical fashion. This was done by using a novel method for the analysis and classification of data based on growing hierarchical self-organizing maps (GHSOM). Self-organizing maps (SOM) have been shown to be successful for the analysis of highly dimensional input data in data mining applications as well as for data visualization. Moreover, the hierarchical architecture of the GHSOM is more flexible than a single SOM in the adaptation process to input data, capturing inherent hierarchical relationships among them. Experimental results show the utility of this approach.

INTRODUCTION

Farmers deal with field patterns that are increasingly split into areas far away from each other and with increased diversity. This is particularly the case for the farmers in the Massif Central (France), where a steady increase in the area used for cattle farming has been observed over the last decade. This contrasts with previous, more stable conditions (55 ha and 1·8 Annual Work Unit (AWU) in 2000 as against 69 ha and 1·8 AWU in 2007 on average for dairy cattle farms (Agreste 2008). Consequently, farmers have to manage fields with constraints that restrict their use. These constraints include: distance from farmstead, slope, small area and altitude. Distance and small area are determinant factors for grazing with dairy cows due to the necessity of going twice a day to the milking parlour (Morlon & Benoit 1990; Brunschwig *et al.* 2006; Andrieu *et al.* 2007). Slope is a major constraint when it comes to mechanization. This is associated with altitude and is a determinant of field use in mountain areas (Fleury *et al.* 1996; Andrieu *et al.* 2007). These constraints are often found on mountain fields and can reduce the season length and land use. Forage production and grazing are often modified by climatic uncertainties (Baumont *et al.* 2008; Mosnier *et al.* 2009). These constraints can increase costs and complicate the matching of fodder production adapted to animal requirements.

Field characteristics are key factors towards managing forage areas as they play an important role with regards to specific farm requirements. This is why research needs to focus on the development of new methods for the management of forage systems. Of special interest are models of livestock farm functioning that consider both temporal and spatial field uses. Martin *et al.* (2009) present an expert discrimination tree based on 53 grassland uses, while Garcia-Launay *et al.* (2012) published a statistical discrimination tree for a cattle farm system based on 1586 field uses.

Land use classification can be thought of as a data mining issue. From this point of view, computational intelligence methods based on unsupervised learning are especially appropriate for understanding or

* To whom all correspondence should be addressed. Email: ejpalomo@lcc.uma.es

https://doi.org/10.1017/S0021859613000737 Published online by Cambridge University Press

extracting unknown information from different data sources. The purpose of unsupervised learning methods is to discover and cluster together similar groups from the input data. These data are usually represented as feature vectors in a highly dimensional space. Data belonging to one group are more similar than data belonging to different groups as defined by a similarity measure. This is also referred to as data clustering (Jain *et al.* 1999), being especially useful when information about the input data is unavailable or unknown.

The self-organizing map (SOM) is an unsupervised learning method that has been used widely for knowledge discovery, data mining, detection of inherent structures in highly dimensional data and mapping this data into a two-dimensional (2D) representation space (Kohonen 1982). This mapping retains relationships within the input data and preserves its topology. The main advantage of this method is the visual understanding of data structures. Different visualization techniques have been used frequently to achieve a better understanding of the data (Vesanto 1999). The SOM has several weaknesses: one is that the number and arrangement of the neurons has to be defined in advance; another is their inability to represent hierarchical relationships. The growing hierarchical self-organizing map (GHSOM) was proposed by Rauber *et al.* (2002) to tackle both limitations. This neural network model has a hierarchical architecture divided into layers, where each layer is composed of different single SOMs with an adaptive architecture that is determined during the unsupervised learning process based on the input data.

In the present paper, the GHSOM model is used for the clustering and visualization of land usage data to achieve a hierarchical clustering. The understanding of this hierarchical clustering is improved by applying different visualization techniques to the maps at each layer. Knowledge of the management of forage production and grazing in grass-based livestock systems is needed to simulate their functioning and propose new practices. The remainder of the present paper is organized as follows. In the next section, a description of the GHSOM model and the training algorithm is provided. Then there follows a brief overview about land usage data and following that is a section presenting an experiment and its results consisting of the analysis and the visualization of land usage data with the GHSOM. The paper ends with a section presenting some conclusions.

HIERARCHICAL SELF-ORGANIZING MODEL

In the present paper, the GHSOM (Rauber *et al.* 2002) was used as a tool to perform hierarchical cluster analysis over land usage. The GHSOM can be considered as an extended version of the standard SOM (Kohonen 1982), where a hierarchy of SOMs is constructed. The main purpose of SOMs is to map high-dimensional data into a 2D representation space, preserving the topology of the data. Thus, understanding of the data is gained by visualizing the resulting map. By using the GHSOM, hierarchical data understanding is also obtained and the size of the architecture does not need to be established in advance.

The GHSOM is an artificial neural network that consists of several growing SOMs (Fritzke 1995) arranged in layers or levels, where the size of the architecture (number of neurons, maps and layers) is automatically determined during the unsupervised learning process, without having to decide this size beforehand. Initially, the GHSOM starts with a single SOM of 2×2 neurons, which is trained with the input data. After training, it can grow by inserting rows or columns of neurons until a certain level of detail in the representation of the data mapped onto the SOM is reached. Once the growing process has finished, the resulting neurons are examined to decide whether they are going to be expanded or not. The idea is to expand into a new map in the next layer of the hierarchy those neurons that represent the most heterogeneous clusters in order to provide a more detailed representation. Once the training process has finished, the final architecture of the GHSOM shows the clusters in which the data were mapped, where data belonging to one cluster are more similar than data belonging to different clusters. Moreover, this architecture reflects the inherent hierarchical relationships between the input data. An example of the architecture of a GHSOM is shown in Fig. 1.

The adaptive growth process of the GHSOM is controlled by means of two parameters, τ_1 and τ_2. These two parameters are used to control the growth of the maps and the neural expansion into new maps of the GHSOM, respectively. The quantity of adaptation depends mainly on the quantization error (qe) of each neuron. The qe is a measure of the dissimilarity of the data mapped onto each neuron, where the higher the value of qe, the higher the heterogeneity of the data cluster. The qe of a

https://doi.org/10.1017/S0021859613000737 Published online by Cambridge University Press

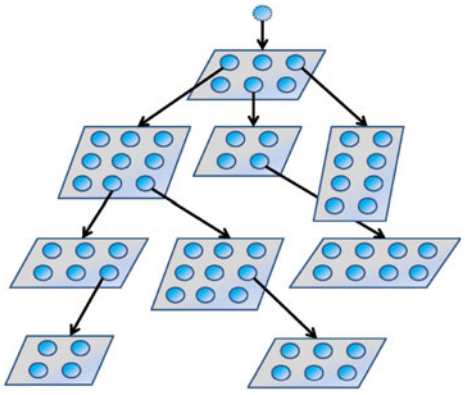


Fig. 1. Example of GHSOM architecture (colour version available online).

neuron i is defined as follows:

$$qe_i = \sum_{x_j \in C_i} \|w_i - x_j\| \tag{1}$$

where C_i is the set of input patterns mapped onto the neuron i, x_j is the jth input pattern from C_i, and w_i is the weight vector of the neuron i.

Once a map m is trained, the possibility that the map can grow must be checked. The quantization error of each neuron (qe_i) of the map m must be computed in order to compute the mean quantization error of the map (MQE_m). If the MQE_m is smaller than a certain fraction τ_1 of the qe of the corresponding parent neuron u in the upper layer, the map stops growing. This stopping criterion for the growth of the map is defined in Eqn (2). Otherwise, the map keeps growing to achieve a better level of representation of the data mapped onto the map, so the smaller the τ_1 parameter chosen the larger the map.

$$MQE_m < \tau_1 \times qe_u \tag{2}$$

The growing of a map is done by inserting a row or a column of neurons between two neurons. These neurons correspond to the neuron with the highest quantization error e and its most dissimilar neighbour d. A row or a column is inserted if these two neurons belong to the same column or row, respectively. The index of the neuron d is computed according to Eqn (3), where $\wedge_e$ is the set of neurons neighbouring e.

$$d = \arg\max_i(\|w_e - w_i\|), \quad w_i \in \wedge_e \tag{3}$$

Initially, the qe at layer 0 must be computed as given in Eqn (4), where w_0 represents the mean of the entire input data I.

$$qe_0 = \sum_{x_j \in I} \|w_0 - x_j\| \tag{4}$$

The initial quantization error (qe_0) measures the dissimilarity of all input data and it is used for the neural expansion process of the GHSOM together with the τ_2 parameter, as given in the stopping criterion of the neural expansion Eqn (5). In this stopping criterion, the quantization error of a neuron i (qe_i) must be smaller than a fraction (τ_2) of the initial quantization error (qe_0) to be a leaf neuron (non-expanded neuron). Otherwise, the neuron is expanded into a new map at the next level of the hierarchy, so the smaller the τ_2 parameter, the deeper the hierarchy.

$$qe_i < \tau_2 \times qe_0 \tag{5}$$

When a new map is created from an expanded neuron, a coherent initialization of the weight vectors of the neuron is used as proposed by Dittenbach *et al.* (2001). This initialization provides a global orientation of the individual maps in the various layers of the hierarchy. Thus, the weight vectors of neurons mirror the orientation of the weight vectors of the neighbour neurons of their parents. The proposed initialization computes the mean of the parent and its neighbours in their respective directions.

A newly created map from its parent neuron is trained as a single SOM. During the training, the set of input patterns are those that were mapped onto the parent neuron. In each iteration t, an input pattern is randomly selected from this data subset. The winning neuron of the map is the neuron with the smallest Euclidian distance to the input pattern, whose index r is defined as:

$$r(t) = \arg\min_i(\|x(t) - w_i(t)\|) \tag{6}$$

The winner's height vector is updated according to Eqn (7). Here, the amount of adaptation is guided by a learning rate α, decreasing in time. In addition to the winner, the winner's neighbours are updated depending on a Gaussian neighbourhood function h_i and their distances to the winning neuron. This neighbourhood function, Eqn (8), reduces its neighbourhood kernel δ during training, being $\|r_c - r_i\|^2$ the distance between neurons c and i within the output space, with r_i representing the 2D coordinates of the neuron i within the grid.

$$w_i(t+1) = w_i(t) + \alpha(t)h_i(t)[x(t) - w_i(t)] \tag{7}$$

https://doi.org/10.1017/S0021859613000737 Published online by Cambridge University Press

Table 1. *Geographical and field use features*

	Features	Description
Geographical	Area	Area of the field (ha)
	Distance	Distance by road between the field and the farmstead (km)
	Altitude	Altitude of the field (m a.s.l.)
	Slope	Proportion of the field area with medium or severe slope
	LowBearing	Proportion of the field area with low soil capacity to bear animals
Field use	StartingUseDate	Starting date for field use (calendar days)
	EndingUseDate	Ending data for field use (calendar days)
	FirstCutDate	Date of first grass cutting (calendar days)
	CutNumber	Number of grass cuttings
	Grazing Days	Number of grazing days (LU × d/ha)
	GrazingDaysMilkedCows	Grazing days by milked cows (LU × d/ha)
	GrazingDaysSucklerCows	Grazing days by suckler cows (LU × d/ha)
	GrazingDaysDryCows	Grazing days by dry cows (LU × d/ha)
	GrazingDaysYoungHeifers	Grazing days by young heifers (LU × d/ha)
	GrazingDaysOldHeifers	Grazing days by old heifers (LU × d/ha)
	GrazingDaysSucklerCalves	Grazing days by suckler calves (LU × d/ha)
	GrazingDaysWeanedCalves	Grazing days by weaned calves (LU × d/ha)
	DistributedForage	Conserved forage distributed at grazing (kg DM/ha)

$$h_i(t) = \exp\left(-\frac{\|r_c - r_i\|^2}{2 \times \delta(t)^2}\right) \quad (8)$$

LAND USAGE DATA

The dataset was organized based on: geographical characteristics, practices and season of forage production, usage (cutting and grazing) and forage supply during grazing.

Description of the traditional salers livestock system

The Traditional Salers Livestock System is located in the Massif Central, France, mainly in the departments of Cantal and Puy-de-Dôme. One mountain breed of cows exploited in these departments is the hardy Salers, which is a dual purpose breed (milk and store production). These cows produce milk concurrently for milking and suckler calves. The calves initiate the milking process. Suckling follows the milking activity. This traditional dual milking production model has been observed in different mountain areas (Teissier 1979).

The survey

A survey in the Salers farms population was done in order to get a representative sample (Garcia-Launay *et al.* 2012). These 72 farms are characterized by medium values for: agricultural area (78 ha), number of cows (43) and low milk quotas (69 000 l/year) compared with the average values observed in France (40 cows with 254 000 litres of milk collected per farm and per year) (Institut de l'Elevage 2008). Milking duration per year varies from a seasonal period of 135 days to all year long. Altitude ranges from 430 to 1400 m a.s.l., which is characteristic of these mountainous areas. The farm systems are based entirely on permanent grasslands with a grazing period duration of 7·5 months on average. Within the sample, 43 farms managed a dual-purpose herd and 29 farms managed both a dual-purpose and a suckler herd. Data were collected for each farmer in 2005 (Agabriel *et al.* 2005). The data concerned the farming system with a focus on animal production and forage management. The information obtained was about herd composition, animal grouping, feeding supply (forage and concentrate) per group throughout the year and also about the total quantities of conserved forage produced and bought. The field was considered as the smallest functional and spatial unit (Thenail & Baudry 2004) with homogeneous land use in 2005. Farmers were asked to characterize each field geographically ($n = 1586$) based on: area, distance to farmstead, slope, altitude and soil capacity (Table 1). Aerial photographs were used to validate the values obtained. The farmers' own perception of the areas/fields with low bearing capacity and with medium or severe slope was also used for validation purposes. It was considered that the

https://doi.org/10.1017/S0021859613000737 Published online by Cambridge University Press

Table 2. *Field use features per dataset*

Dataset	Field use features
Cut only	EndingUseDate (calendar days) FirstCutDate (calendar days) CutNumber
Cut and grazed	StartingUseDate EndingUseDate FirstCutDate CutNumber
Grazed only	Grazing Days GrazingDaysMilkedCows GrazingDaysDryCows GrazingDaysSucklerCows GrazingDaysYoungHeifers GrazingDaysOldHeifers GrazingDaysSucklerCalves GrazingDaysWeanedCalves DistributedForage

farmers' perception had a higher correlation with the grassland use than measured variables.

A detailed cutting and grazing schedule was drawn up for each field (Table 1) and reports produced, including: cutting dates, type of conserved forage harvested, entrance and exit dates of animal groups, and quantity of forage supplied at grazing. Fields that were cropped ($n = 23$), used by other farmers ($n = 28$) or abandoned ($n = 35$) were excluded from the present study.

RESULTS

In order to demonstrate the application of GHSOM in the field of land use classification, several experiments and results are described in this section. These experiments consist of the analysis and data visualization of geographical and field use characteristics and cutting and/or grazing practices in three general groups of fields: cut only, cut and grazed and grazed only fields. Land use analysis and subsequent visualization of the resulting data was based on GHSOM models. The resulting data visualizations are useful to help characterize the types of grassland use in a mountain cattle farm system and to link them to the geographical characteristics of the fields. This provides a conceptual model of grassland use that can be easily adapted to counselling and modelling needs.

Data preparation

For each of the three datasets, both the field use and the geographical features were taken into account for the cluster analysis. A description of the field use and geographical features utilized in these datasets is given in Table 1. The five geographical features are present in the three datasets. These are: area, distance, altitude, proportion of area with medium or severe slope and with low bearing. Some datasets contained missing values, which were removed from the datasets. Since the aim is to cluster the data samples, the class labels were not included. The first dataset corresponding to cut only fields contained a total of 112 samples and eight features, with three field use features and five geographical features. The second dataset (cut and grazed) had a total of 660 samples with nine features (four field use and five geographical). Finally, the third dataset (grazed only) contained 746 samples with 14 features (nine from field use and five geographical). The field use features present in each dataset are shown in Table 2.

Data visualization

The three datasets were used to train the GHSOM model in order to build a hierarchical clustering model of the data. The τ_1 and τ_2 parameters were set to 0·1, since this achieves a small architecture of two layers that can be easily analysed and understood. Ten runs were performed for each dataset, generating ten architectures for each one. All the architectures obtained by training with the same dataset were similar to each other. However, they were not exactly the same since the input samples were presented randomly to the neural network. Therefore, the architecture that achieved the best level of clustering, considered to be the one with the minimum sum of *qe* of the hierarchical model (see previously), was selected in order to analyse the results of each dataset.

For the sake of simplicity, only the visualizations corresponding to the first dataset are shown in the present paper. Thus, the hierarchical 3D architecture and its projection in a 2D map for the selected model from the first dataset are shown in Figs 2 and 3, respectively. In Fig. 2, the architecture has two layers and three maps in the second layer. All the obtained architectures for the three selected models have two layers with three or four maps in the second layer, so the analysis performed in the present paper for the first dataset is valid for the two remaining datasets. Each sphere represents a neuron. Numbers were assigned to each neuron in order to identify them. The expanded neurons are represented with darker shades and without horizontal lines. An arrow going

https://doi.org/10.1017/S0021859613000737 Published online by Cambridge University Press

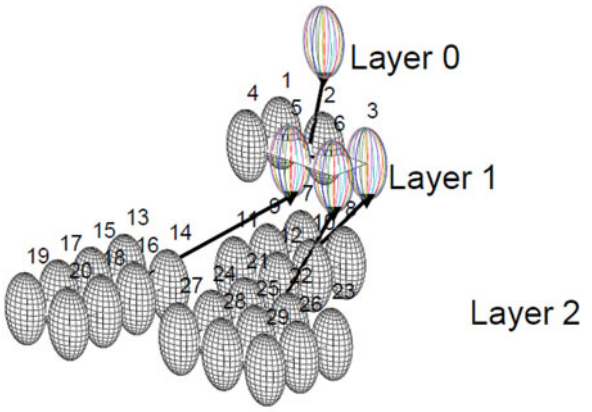


Fig. 2. Three-dimensional architectures for the cut only dataset. Each sphere represents a neuron and identification numbers were assigned to each neuron. The expanded neurons are represented with darker shades and without horizontal lines (colour version available online).

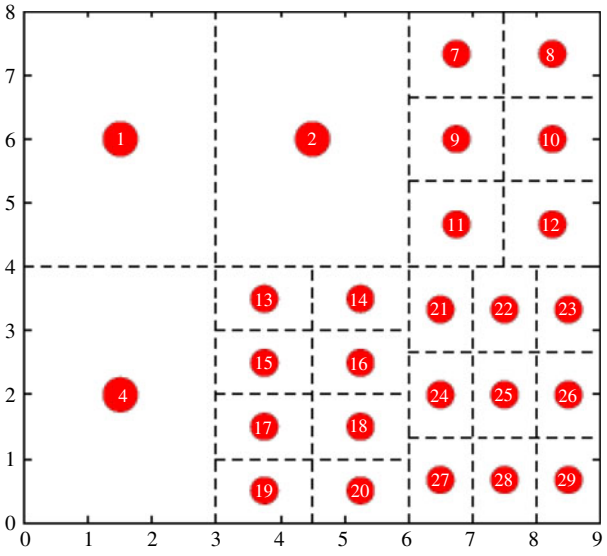


Fig. 3. Two-dimensional projections of the hierarchical architectures for the cut only dataset. Each square represents a neuron or a map, where the smaller the size of the square, the deeper the level of the hierarchy of the neuron or map. Thus, the biggest square represents the neuron at layer-0 map and the smallest one a neuron at layer 2. Numbers were assigned to each neuron (colour version available online).

out from the neuron indicates the map into which it was expanded. The 2D projections of these hierarchies can help in visualizing the neural subdivision at a glance. In Fig. 3, each square represents either a neuron (if it contains a circle in its centre) or a map (if it is subdivided into more squares). The smaller the size of the square the deeper the layer it belongs to

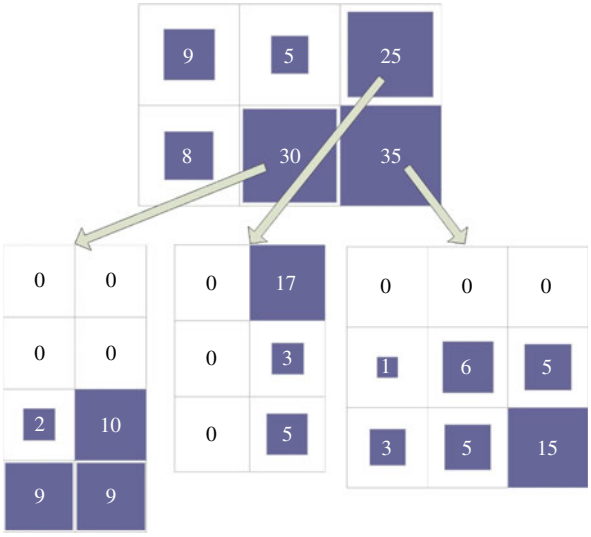


Fig. 4. Input data hits for the architecture corresponding to the cut only dataset. Each square represents a neuron with its number of samples associated and also the relative number of samples by means of the size of a coloured patch. The neurons with a larger number of samples are the ones that have been expanded (indicated with an arrow). Neurons without any sample associated are considered dead neurons (colour version available online).

(the biggest square is the map at layer zero). It can be seen in these plots how for the first architecture, neurons 3, 5 and 6 were expanded into three maps of 3×2, 4×2 and 3×3 neurons, respectively. These two representations of the hierarchical architecture provide a better understanding of the resulting clustering for each dataset corresponding to different cutting and/or grazing practices.

By observing the obtained architectures, the relationships and arrangement among clusters can be analysed, although information about the input data mapped into the clusters is not reflected. In order to show the relationship between the input data and the clusters, more visualization techniques are used. One of these techniques is to plot the input data hits, which shows the number of samples mapped onto each cluster of the architecture. The distribution of samples into clusters for the obtained hierarchy corresponding to the first dataset is given in Fig. 4. The relative number of samples for each neuron is also shown by means of the size of a coloured patch. Note that those neurons with larger numbers of mapped data are expanded. In this plot, it can be seen that for the cut only field, from the 112 samples initially mapped, 25, 30 and 35 were expanded into three new maps in the second layer. In the maps from the second layer of the architecture,

https://doi.org/10.1017/S0021859613000737 Published online by Cambridge University Press

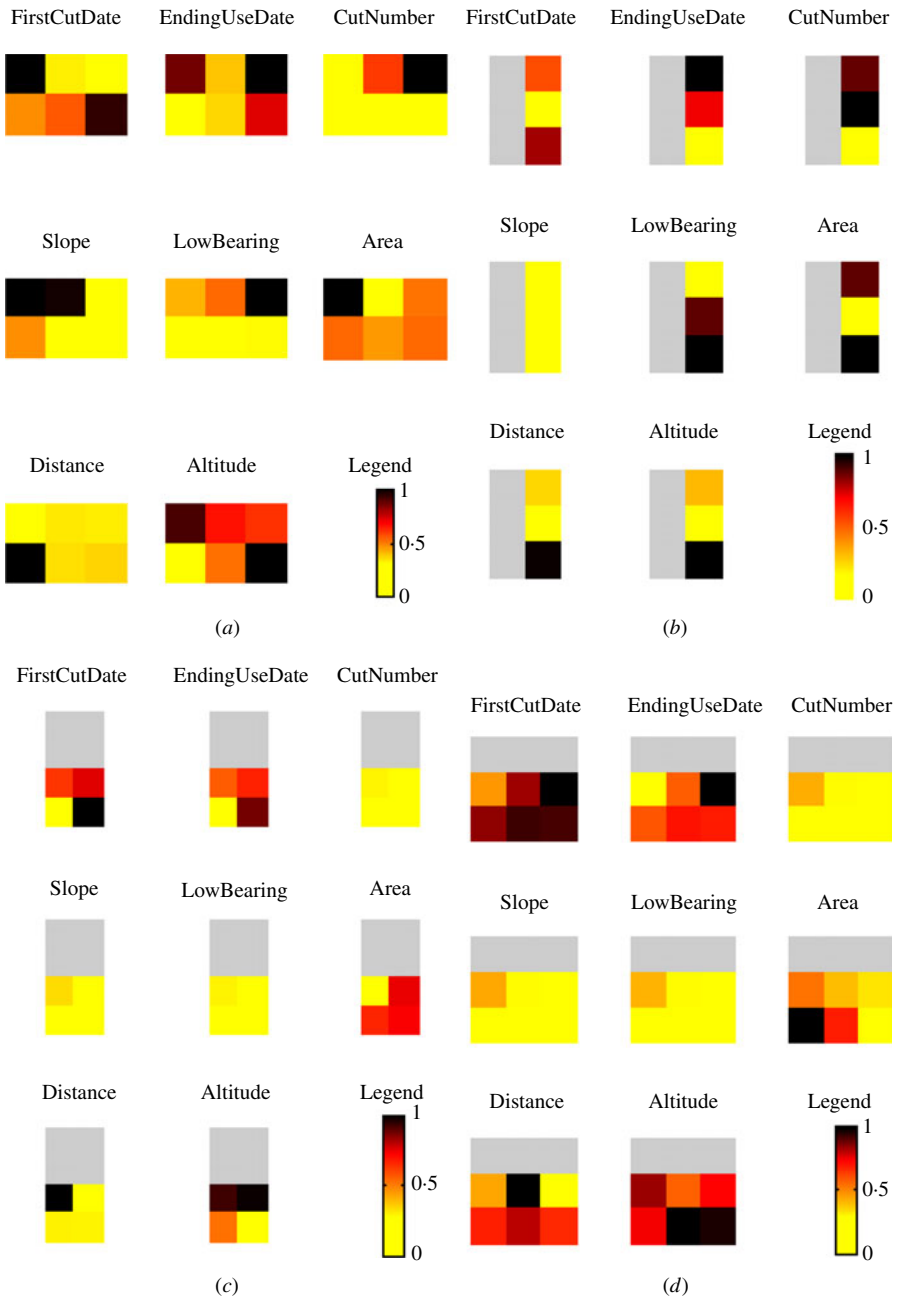


Fig. 5. Component planes for the cut only dataset: (*a*) layer-1 map, (*b*) layer-2 first map, (*c*) layer-2 second map and (*d*) layer-2 third map. Larger weights are represented by darker shades. A colour legend is shown, where the values of the component planes are normalized between 0 and 1. Dead neurons are coloured in grey (colour version available online).

neurons with no samples associated can be detected. These neurons are considered 'dead' and do not provide any information about the clustering performed. Thus, they can be ignored from now on.

Another useful visualization technique to obtain more information about the data mapped into the clusters is the plot of the component planes. This shows the distribution of the feature values in order to see the spread of data from each feature (or component) in all map neurons. By comparing the corresponding component planes for each feature, possible correlations among features can be discovered. The component planes of the maps corresponding to the first group of field are given in Fig. 5. In the plots, there is a component plane per feature, where larger weights (higher values of a feature) are represented by darker shades. A colour legend shows the values of the component planes normalized

https://doi.org/10.1017/S0021859613000737 Published online by Cambridge University Press

Table 3. *Values of the component planes from the cut only field architecture*

Map	Neuron	FirstCutDate	EndingUseDate	CutNumber	Slope	LowBearing	Area	Distance	Altitude
L1/M1	1	199	210	1·0	0·953	0·05	2·2	0·74	980
	2	160	175	1·3	0·918	0·09	0·94	1·5	808
	3	159	222	1·8	0·0	0·31	1·3	1·3	779
	4	168	169	1·0	0·21	0·0	1·3	18	600
	5	172	173	1·0	0·0	0·0	1·2	1·8	724
	6	195	199	1·0	0·0	0·002	1·3	2·2	1042
L2/M1	2	159	241	1·9	0·0	0·0001	1·4	1·4	765
	4	150	208	2·2	0·0	0·81	0·80	1·4	741
	6	167	172	1·1	0·0	1·0	1·5	1·8	916
L2/M2	5	166	167	1·0	0·047	0·0031	0·8	7·5	840
	6	171	172	1·0	0·0	0·0	1·2	1·5	869
	7	152	153	1·0	0·0	0·0	1·1	1·6	673
	8	187	188	1·0	0·0	0·0	1·2	1·6	595
L2/M3	4	171.	176	1·1	0·052	0·023	1·9	1·3	1022
	5	189	191	1·0	0·002	0·0009	1·1	3·3	883
	6	201	222	1·0	0·0	0·0	0·65	0·86	950
	7	191	192	1·0	0·0	0·0	5·8	1·9	958
	8	197	198	1·0	0·0	0·0	2·8	2·4	1130
	9	196	197	1·0	0·0	0·0	0·37	1·9	1110

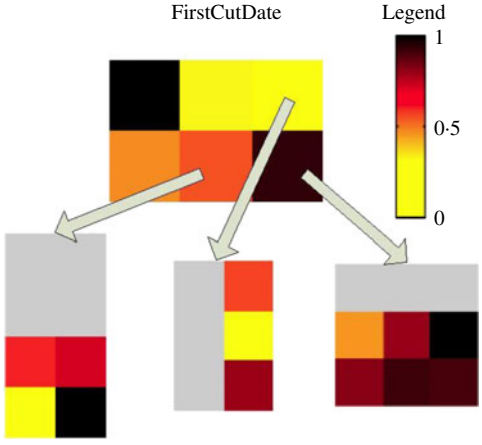


Fig. 6. Component planes for the 'FirstCutDate' feature corresponding to the architecture of the cut only dataset. Larger weights are represented by darker shades. A colour legend is shown, where the values of the component planes are normalized between 0 and 1. Dead neurons are coloured in grey (colour version available online).

between 0 and 1. Dead neurons are coloured in grey and must be ignored in the analysis since they do not represent any data cluster. By observing these plots, no correlations are detected among features, indicating that the features were selected properly. In Fig. 6, a detail of the component planes for the 'FirstCutDate' feature is given, where the hierarchical relations of the component planes can be better perceived.

Apart from detecting possible correlations among features, more information can be extracted from these plots. This information is summarized in Tables 3–5 for the cut only, cut and grazed and grazed only field groups, respectively. Here, it can be seen that the values representing all the data mapped onto each cluster in each field group.

Considering the cut only fields (Table 3), the L2/M3 map could be characterized as fields with late cut and relatively elevated altitude (cf. Neuron 9), the L2/M2 map as fields with early cut (cf. Neuron 5), and the L2/M1 map as fields with two cuts and/or low bearing (cf. Neuron 4), while L1/M1 map appears to be more heterogeneous.

For the cut and grazed fields (Table 4), the L2/M4 map could be characterized as fields with long periods of use, early first cut and late ending date, and situated at low altitude (cf. Neuron 9), the L2/M3 map as fields with late first cut, medium usage end date and located at elevated altitude (cf. Neuron 6), the L2/M2 map as fields with a longer period of use, early grazing before a first cut, a medium ending date, and situated at low altitude (cf. Neuron 5), the L2/M1 map as fields with grazing before a first cut, medium ending date, high proportion of area with medium or severe slope and situated at medium altitude (Neuron 5) and L1/M1 map as fields with grazing before an early first cut, a late ending date, with slope or low bearing, a relatively

https://doi.org/10.1017/S0021859613000737 Published online by Cambridge University Press

https://doi.org/10.1017/S0021859613000737 Published online by Cambridge University Press

Table 4. *Values of the component planes from the cut and grazed field architecture*

Map	Neuron	FirstCutDate	StartingUseDate	EndingUseDate	CutNumber	Slope	LowBearing	Area	Distance	Altitude
L1/M1	1	178	138	298	1·1	0·98	0·011	2·8	1·8	898
	2	183	104	294	1·0	0·0082	0·011	4·2	1·2	812
	3	182	174	294	1·2	0·0054	0·0054	3·0	1·8	1040
	4	180	145	317	1·0	1·0	1·0	5·1	1·8	780
	5	177	144	302	1·1	0·0	0·98	3·1	1·5	844
	6	164	164	311	1·2	0·0035	0·00	2·4	2·7	714
L2/M1	1	176	120	213	1·1	1·00	0·0	3·7	0·72	1013
	2	196	115	311	1·1	1·00	0·0	3·0	0·80	993
	3	162	136	304	1·2	1·00	0·0	2·1	2·9	655
	4	175	173	309	1·2	1·00	0·016	2·8	2·4	1037
	5	182	140	299	1·1	0·77	0·020	2·2	1·1	963
	6	179	135	284	1·0	0·50	0·0044	0·78	0·23	918
	8	172	133	311	1·0	0·67	0·50	4·8	1·2	800
	9	180	131	304	1·1	0·34	0·66	4·1	1·5	812
L2/M2	1	184	98	326	1·0	0·0	0·0	3·8	1·0	643
	2	166	82	277	1·4	0·0	0·0	2·1	10	763
	3	182	105	183	1·0	0·0	0·0	3·6	1·2	888
	4	195	102	297	1·0	0·33	0·0054	1·9	1·0	676
	5	188	107	285	1·0	0·0	0·0	2·7	0·55	705
	6	184	111	303	1·0	0·0053	0·0073	3·8	0·65	1002
	7	178	142	306	1·1	0·65	0·65	3·7	1·7	841
L2/M3	1	200	132	300	1·0	0·012	0·013	2·9	0·74	1086
	2	170	130	295	2·0	0·0002	0·0001	1·9	0·32	1008
	3	172	173.	303	2·0	0·0	0·0	3·3	2·5	1026
	4	166	167	306	1·0	0·0	0·0	4·0	1·1	984
	5	175	168	252	1·0	0·0	0·0	2·1	1·2	1011
	6	197	198	291	1·1	0·0	0·0001	6·3	20	1089
	7	172	170	319	1·0	0·14	0·34	4·5	0·62	992
	8	190	191	312	1·0	0·0	0·0001	2·5	1·3	961
	9	190	191	295	1·0	0·0021	0·0072	2·7	1·2	1133
L2/M4	2	168	169	277	1·0	0·034	0·0	2·3	8·7	653
	3	177	177	319	1·0	0·0048	0·0	2·7	1·2	667
	5	160	159	312	1·0	0·0	0·0	1·8	0·95	835
	6	145.	141	310	1·0	0·0	0·0	3·2	0·90	636
	9	157	158	313	2·0	0·0	0·0	1·6	4·1	766

https://doi.org/10.1017/S0021859613000737 Published online by Cambridge University Press

Table 5. *Values of the component planes from the grazed only field architecture*

Map	Neuron	GDM Cows	GDD Cows	GDS Cows	GDY Heifers	GDO Heifers	GDS Calves	GDW Calves	Grazing Days	DForage	Slope	Low Bearing	Area	Distance	Altitude
L1/M1	1	55	9·1	108	50	21	26	1·5	271	1516	0·99	0·99	3·8	1·6	845
	2	45	4·0	64	143	26	2·7	0·20	286	723	0·084	0·50	3·6	4·2	1080
	3	161	9·7	35	58	27	78	4·7	418	2146	0·011	0·0014	3·3	2·3	706
	4	102	7·1	34	60	34	52	9·8	329	1015	1·0	0·0072	3·3	3·6	888
	5	87	3·3	51	39	42	24	5·5	283	999	0·045	0·0027	5·4	3·8	1070
	6	135	5·7	36	39	65	59	3·5	357	976	0·004	1·0	3·2	1·9	803
L2/M1	1	22	0·01	5·9	23	0·06	749	47	1131	4909	0·0	0·00	1·1	0·11	737
	2	47	9·4	14	4·7	7·0	24	0·22	534	22078	0·0	0·00	12	0·44	739
	3	31	3·8	65	44	66	9·6	1·6	241	979	0·023	0·0023	3·6	4·41	690
	4	410	4·7	2·4	4·0	1·3	24·9	1·6	450	1666	0·0039	0·00	3·1	0·39	709
	5	0·01	0·0	0·11	427	9·3	0·74	0·54	438	245	0·0	0·0	1·4	1·74	764
	6	294	128	0·12	0·01	26	9·6	3·2	461	632	0·0	0·0001	3·0	0·78	715
L2/M2	1	84	0·0	0·02	160	4·9	0·39	0·0	249	168	1·00	0·43	11	0·36	954
	4	15	3·9	81	35	67	79	15	348	948	1·00	0·00	3·6	3·2	698
	5	102	4·4	30	17	41	65	4·8	273	673	1·00	0·0068	3·6	2·3	1040
	6	108	0·47	20	24	7·2	4·0	0·40	165	254	0·64	0·028	6·6	1·8	1220
	7	411	28	9·4	1·6	4·6	11	3·0	469	2838	1·00	0·00	3·8	0·6	740
	8	31	0·44	38	5·8	98	23	0·09	214	3423	1·00	0·0024	12	67	1071
	9	1·6	1·6	0·43	222	14	0·23	0·0	239	835	1·00	0·00	2·1	2·4	914
L2/M3	5	67	9·5	62	39	30	4·7	0·06	232	405	0·40	0·0015	3·2	1·9	1025
	6	115	5·2	45	3·4	46	46	6·9	307	1330	0·0	0·0021	3·5	1·2	1049
	7	0·18	0·13	6·1	200	22	0·03	0·0	229	185	0·021	0·0	2·9	3·8	1075
	8	79	0·49	116	7·3	35	0·33	0·01	238	1116	0·34	0·0004	19	1·7	1139
	9	100	1·9	46	2·5	43	2·5	0·12	203	1325	0·0	0·0082	18	17	1166

large area and long distance from farmstead and medium altitude (cf. Neuron 4).

For the grazed only fields (Table 5), the maps were characterized as follows: L2/M3 map as fields used by milking cows and suck-ling cows, medium forage distribution and grazing days and situated at elevated altitude (cf. Neuron 8), L2/M2 map as fields grazed by milking cows, heterogeneous grazing days and forage distribution, with high proportion of area with medium or severe slope and relatively large area (cf. Neuron 5), L2/M1 map mainly grazed by milking cows, with high grazing days and forage distribution, situated at small distance from farm-stead and low altitude (cf. Neuron 4), and L1/M1 map as fields more grazed by suckling cows and heifers, with high grazing days and forage distribution, and situated at long distance from farm-stead and medium altitude (cf. Neuron 2).

CONCLUSIONS

Geographical characteristics are key discriminators of grassland use. A hierarchical visualization of land usage data was provided using a GHSOM neural network. The GHSOM is composed of several independent growing SOMs, arranged in a hierarchical architecture, that are automatically established during the unsupervised learning process. As a consequence, this hierarchical architecture provides a more flexible adaptation to input data than a single SOM and a better capture of the relationships among them. Therefore, the improvement in data modelling provides a better visualization and understanding of the input data. By using the GHSOM for land usage data, the provided hierarchy of SOMs can be analysed to extract relevant information about the mapped data. This may aid agronomists and farmers to better understand hidden relationships in the datasets.

In the present paper, a dataset obtained by capturing data from 1586 was utilized to train the GHSOM algorithm. Different visualization techniques were used to represent different maps. After considering all the data plots together with the hierarchical architecture, a better insight of the data was achieved and several clusters could be identified along the hierarchy. The proposed hierarchical model of grassland use shows that a combination of geographical characteristics may be associated with several types of grassland use. The use of these fields may be adapted according to weather conditions and herd requirements during the grazing season. The map obtained highlighted groups that could be characterized by types of field use related to some geographical characteristics, while the neurons enabled a better characterization of this relationship. This way to classify field uses could be of interest as input in a farm simulator to specify the possible uses of fields associated to their geographical characteristics. This is particularly interesting in case of *in silico* experiment or in case of complete reorganization of grazing and forage system or of farming systems. Further investigation will consider the influence of field pattern characteristics on these relationships.

REFERENCES

Agabriel, C., Sibra, C., Journal, C. & Coulon, J. (2005). Interest and data analysis of survey in livestock farming: reflection over 15 years of practice. *Rencontres autour des Recherches sur les Ruminants* **12**, 331–334.

Agreste (2008). *Caractéristiques* Générales des Exploitations, France Métropolitaine. Castanet Tolosan, France: Ministère de l'Agriculture, de l'Agroalimentaire et de la Forêt.

Andrieu, N., Josien, E. & Duru, M. (2007). Relationships between diversity of grassland vegetation, field characteristics and land use management practices assessed at the farm level. *Agriculture, Ecosystems and Environment* **120**, 359–369.

Baumont, R., Deux, N., Farruggia, A. & Jouven, M. (2008). Simulation of the sensitivity and adaptation of beef cattle farming systems to extreme climatic events based on permanent pasture. *Rencontres autour des Recherches sur les Ruminants* **15**, 209.

Brunschwig, G., Josien, E. & Bernhard, C. (2006). Contraintes géographiques et modes d'utilisation des parcelles en élevage bovin laitier et allaitant. *Fourrages* **185**, 83–95.

Dittenbach, M., Rauber, A. & Merkl, D. (2001). Recent advances with the growing hierarchical self-organizing Map. In *Advances in Self-Organising Maps (WSOM)* (Eds N. Allinson, H. Yin, L. Allinson & J. Slack), pp. 140–145. London: Springer.

Fleury, P., Dubeuf, B. & Jeannin, B. (1996). Forage management in dairy farms: a methodological approach. *Agricultural Systems* **52**, 199–212.

Fritzke, B. (1995). Growing grid – a self-organizing network with constant neighborhood range and adaptation strength. *Neural Processing Letters* **2**, 9–13.

Garcia-Launay, F., Sibra, C., Molenat, H., Agabriel, C. & Brunschwig, G. (2012). Grassland use in mountain bovine systems according to a hierarchy of geographical determinants. *Journal of Agricultural Science, Cambridge* **150**, 203–217.

Institut de l'Elevage (2008). *Les Chiffres Clés 2008: Productions Bovines Lait & Viande*. Paris, France: Institut de l'Elevage.

Jain, A. K., Murty, M. N. & Flynn, P. J. (1999). Data clustering: a review. *ACM Computing Surveys* **31**, 264–323.

https://doi.org/10.1017/S0021859613000737 Published online by Cambridge University Press

Kohonen, T. (1982). Self-organized formation of topologically correct feature maps. *Biological Cybernetics* **43**, 59–69.

Martin, G., Hossard, L., Theau, J. P., Therond, O., Josien, E., Cruz, P., Rellier, J. P., Martin-Clouaire, R. & Duru, M. (2009). Characterizing potential flexibility in grassland use. application to the French Aubrac area. *Agronomy for Sustainable Development* **29**, 381–389.

Morlon, P. & Benoit, M. (1990). Etude méthodologique d'un parcellaire d'exploitation agricole en tant que système. *Agronomie* **10**, 499–508.

Mosnier, C., Agabriel, J. & Lherm, M. (2009). Dynamics of suckler cow farms under stochastic crop yields: a recursive discrete stochastic programming approach. In *Proceedings of the Conference on Integrated Assessment of Agriculture and Sustainable Development: Setting the Agenda for Science and Policy (AgSAP 2009), Hotel Zuiderduin, Egmond aan Zee, The Netherlands, 10–12 March 2009* (Eds M. van Itterson, J. Wolfe & G. van Laar), pp. 264–265. Wageningen, The Netherlands: Wageningen University and Research Centre.

Rauber, A., Merkl, D. & Dittenbach, M. (2002). The growing hierarchical self-organizing map: Exploratory analysis of high-dimensional data. *IEEE Transactions on Neural Networks* **13**, 1331–1341.

Teissier, J. H. (1979). Relations entre techniques et pratiques. *Bulletin INRAP* **38**, 1–19.

Thenail, C. & Baudry, J. (2004). Variation of farm spatial land use pattern according to the structure of the hedgerow network (bocage) landscape: a case study in northeast Brittany. *Agriculture Ecosystems and Environment* **101**, 53–72.

Vesanto, J. (1999). SOM-based data visualization methods. *Intelligent Data Analysis* **3**, 111–126.

https://doi.org/10.1017/S0021859613000737 Published online by Cambridge University Press